Journal of Electronic Research and Application, 2026, Volume 10, Issue 4
http://ojs.bbwpublisher.com/index.php/JERA
Online ISSN: 2208-3510
Print ISSN: 2208-3502

From Lithium Plating Onset to Severe Deposition: A Three-Electrode-Based Grading of Lithium Plating

Yu Fan*

School of Mechanical Engineering, University of Shanghai for Science and Technology, Shanghai 200093, China.

***Corresponding author**: Yu Fan, 232191389@st.usst.edu.cn

* **Author to whom correspondence should be addressed.**

Abstract: Lithium (Li) plating is a critical barrier to fast charging in lithium-ion batteries as it accelerates degradation and compromises safety. Nevertheless, in practice, the determination of the onset of plating is not enough; real-time monitoring of plating severity has more value in charging control. A lithium plating grading system is developed based on the development of the negative-electrode potential in a three-electrode pouch cell. Operando monitoring of the graphite anode potential at charging enables determination of the shift between stable Li intercalation and plating-prone conditions and correlation with various levels of metallic lithium deposition. Auxiliary dynamic electrochemical impedance spectroscopy (DEIS) is used to investigate the development of the entire interfacial response. Lithium plating can be divided into four classes under combined post-mortem SEM, EDS, and XPS analysis; namely, plating-free, mild, moderate, and severe. The findings indicate that the higher the anode potential becomes more negative, the greater the intensity of the Li deposition and increasing modifications in the surface morphology and interfacial chemistry. This paper presents a method of severity-based diagnosis of lithium plating and gives a sound base upon which rapid-charging risk estimation and optimization of charging protocols can be executed.

Keywords: Lithium-ion battery; Fast charging; Anode potential; Severity grading; Three-electrode cell

Online publication: May 21, 2026

1. Introduction

Lithium-ion batteries require fast charging in electric vehicles and other high-power devices, but lithium plating on graphite anodes is still a significant concern since it hastens degradation and raises the safety risk level [1–4]. The current diagnostic techniques may be generally subdivided into voltage, multi-signal, operando, and impedance methods. Nevertheless, the majority of the works are dedicated to the onset of

plating instead of their level of seriousness, and practical battery management should be done using severity-based assessment since various levels of plating have varying degrees of degradation and safety results [5–12]. In order to fill this gap, the present work introduces a four-stage lithium plating classification system that relies on operando measurement of the negative-electrode potential in a three-electrode pouch cell and DEIS as a secondary probe and SEM/EDS/XPS as a post-mortem check (**Figure 1**).

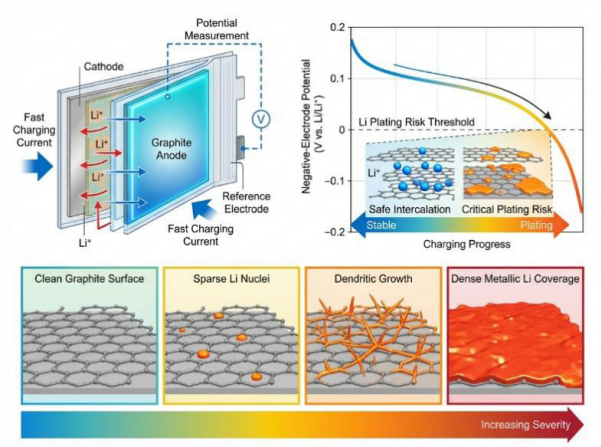

Figure 1. Grading of lithium plating severity.

2. Experimental methodology

Commercial 1 Ah lithium-ion pouch cells were used in this study. A three-electrode configuration was constructed by inserting a lithium titanate (LTO)-based reference electrode close to the graphite anode to enable operando measurement of the negative-electrode potential while minimizing internal voltage-gradient error. The electrolyte was 1 M $LiPF_6$ in EC/EMC (3:7 by mass) with 2 wt% VC additive. After assembly, the cells were rested for wetting and then formed to stabilize the interfaces and activate the reference electrode.

Before testing, the cells were discharged to 0% SOC and rested to reach open-circuit equilibrium. Galvanostatic charging was then performed at 0.1C, 1C, 2C, and 4C at 25 ± 1 °C. During charging, the graphite negative-electrode potential was continuously recorded against the LTO reference electrode. DEIS measurements were carried out using an Autolab PGSTAT302N workstation by superimposing a small AC perturbation on the charging current. After charging, selected cells were disassembled in an Ar-filled glove box, and the harvested graphite electrodes were rinsed with dimethyl carbonate and dried. SEM, EDS, and XPS were used for post-mortem characterization.

2.1. Fast-charging protocols and negative-electrode potential measurements

Prior to testing, the cells were discharged to 0% SOC and allowed to rest until stable open-circuit conditions were achieved. Subsequently, galvanostatic charging was carried out at 0.1C, 1C, 2C, and 4C within a temperature-controlled chamber at 25 ± 1 °C. Potential of the graphite negative electrode was measured against the LTO reference electrode during the whole process of charging. The change in the negative-electrode potential with SOC served as the main characteristic of the shift between normal intercalation and plating-prone states.

2.2. Dynamic electrochemical impedance spectroscopy

An Autolab PGSTAT302N electrochemical workstation was used in measuring DEIS. The impedance response was measured during the charging of the battery with a small AC perturbation on the charging current in galvanostatic mode over a chosen frequency range. In this paper, DEIS was used as a supplementary characterization approach to explore the rate-dependent changes of interfacial response at the cell level.

2.3. Post-mortem characterization

Selected charged cells were subsequently disassembled in an Ar-filled glovebox. Graphite electrodes that were harvested were washed in dimethyl carbonate and dried before they were characterized. SEM, EDS and XPS were used to examine the surface morphology, elemental composition and surface chemistry respectively. Post-mortem analyses were utilized to confirm the potential-based lithium plating severity grading framework.

3. Results and discussion

3.1. Evolution of negative-electrode potential under different charging rates

The negative-electrode potential as a function of SOC during charging at 0.1C, 1C, 2C, and 4C is illustrated in **Figure 2**. It can be clearly seen that the rate is dependent. The decrease at 0.1C is slow and stays within a fairly constant range, which indicates intercalation-dominated behaviour and acts as a baseline without plating. The potential declines more quickly at 1C which is indicative of higher anode polarization. The potential decreases more quickly and achieves lower values at earlier SOC at 2C, implying that the anode has entered a high-risk state earlier. At 4C the potential also drops abruptly at low SOC, indicating both early strong polarization and a significantly greater chance of metallic Li-plating.

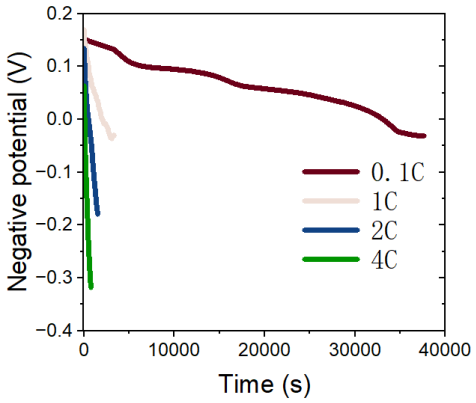

Figure 2. Negative-electrode potential evolution during charging.

The findings point to the fact that lithiation plating ought not to be viewed as a single-threshold phenomenon but rather as a gradual shift towards safe intercalated conditions to dangerous depositing conditions. The negative-electrode potential enters the plating-prone region sooner and further as the rate of charging becomes higher. Because the practical electrodes are spatially heterogeneous, there may be limited excursion into this region and it will signify only localized nucleation, but earlier, deeper and prolonged

residence can lead to widespread deposition. Hence, the negative-electrode potential is a more informative indicator than just the charging rate and is used to grade severity.

3.2. Construction of a lithium plating severity grading framework

According to the level of negative-electrode potential deviation and its correlation with post-mortem observations, there were four levels of lithium plating:

(1) The potential of the negative electrode remains in the stable intercalation region during charging and the majority of lithium is stored by reversible insertion into graphite;

(2) Grade I (mild plating): The potential starts to penetrate into the plating-prone area; however, the penetration is restricted in terms of depth and time; it is assumed that the deposition will be localized and thin;

(3) Grade II (moderate plating): The potential invades the plating-susceptible area sooner and stays there more noticeably, which means that a larger and more spatially distributed deposition of metallic Li is formed;

(4) Grade III (severe plating): The potential is entering the dangerous low-potential area early and deeply, which means that the conditions favoring plating are very high and long-lasting with the large-scale deposition of material on the surface.

The model focuses on gradual risk development instead of binary discovery. It is intended to offer a physical structure that can be interpreted to compare the severity of plating between similar cell systems, but it does not aim at setting a universal potential level of all graphite-based cells. The severity of lithium deposition increases with how early, deep, and long the negative-electrode potential stays in the plating-prone region.

3.3. DEIS as an auxiliary probe of interfacial response

The DEIS results of charging at various rates are displayed in **Figure 3**. Though DEIS is not a main evaluation parameter, it gives supplementary data about the development of the total interfacial behavior. At 0.1C charging, the impedance response is fairly low, which can be explained by steady intercalation and minimal polarization. Spectra change at 1C, which indicates growing kinetic and transport restrictions. At 2C and 4C, the spectral evolution has a significantly greater amplitude, signifying increased polarization and more turbulent interfacial dynamics.

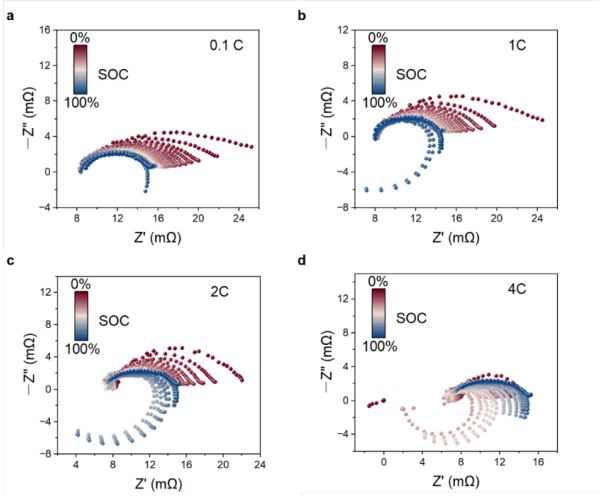

Figure 3. DEIS during charging at different C-rates. (a) 0.1C. (b) 1C. (c) 2C. (d) 4C.

Impedance is a composite reaction of the entire cell, but it cannot give the same electrode-specific details like negative-electrode potential. However, its regular development with charge rate is in good conformity with the potential-related explanation of the growth in anode polarization and plating intensity.

3.4. Ex situ validation of plating grades by SEM and EDS

3.4.1. SEM analysis of lithium plating morphology

SEM observations show a clear progression of graphite surface morphology with increasing plating severity (**Figure 4**). Under the Grade 0 condition, the graphite surface remains largely intact and no obvious metallic deposits are observed, confirming plating-free behavior.

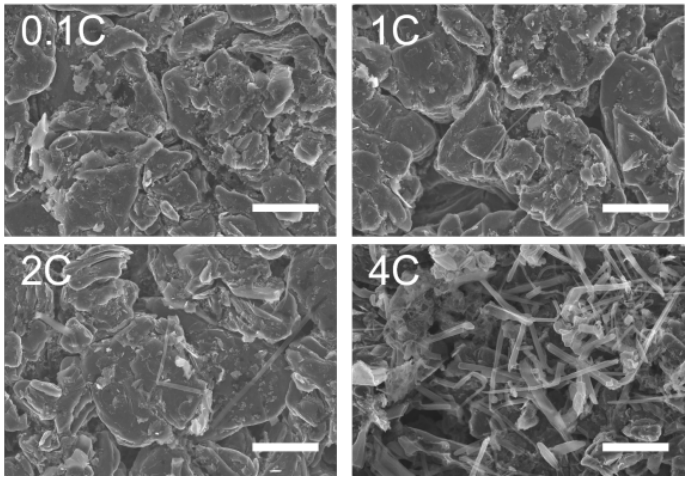

Figure 4. The SEM images of ex situ characterization of the structural evolution under varying degrees of lithium plating severity. The scale bar corresponds to 5 μm.

For Grade I, sparse and localized protrusions or needle-like features appear on the graphite surface, indicating the onset of metallic Li nucleation in the most polarized regions. Under Grade II conditions, the density and spatial distribution of deposited features increase markedly, and the surface exhibits more continuous and partially connected deposits, indicating more developed surface accumulation. In Grade III conditions, there is heavy deposition of the graphite surface which is very much disrupted in morphology and in certain areas it has clear dendritic features .

The SEM findings can be directly related to the suggested four-stage model, indicating that there is a shift in the graphite that was initially intact into localized nuclei followed by denser connected deposits and eventually widespread surface coverage.

3.4.2. EDS analysis of surface elemental evolution

The findings of EDS are also able to confirm the grading system since they display systematic changes in the composition as the severity increases (**Figure 5**). Carbon is the main component at the surface when Grade 0 is present, which agrees with the preserved morphology of graphite and minimal side reactions.

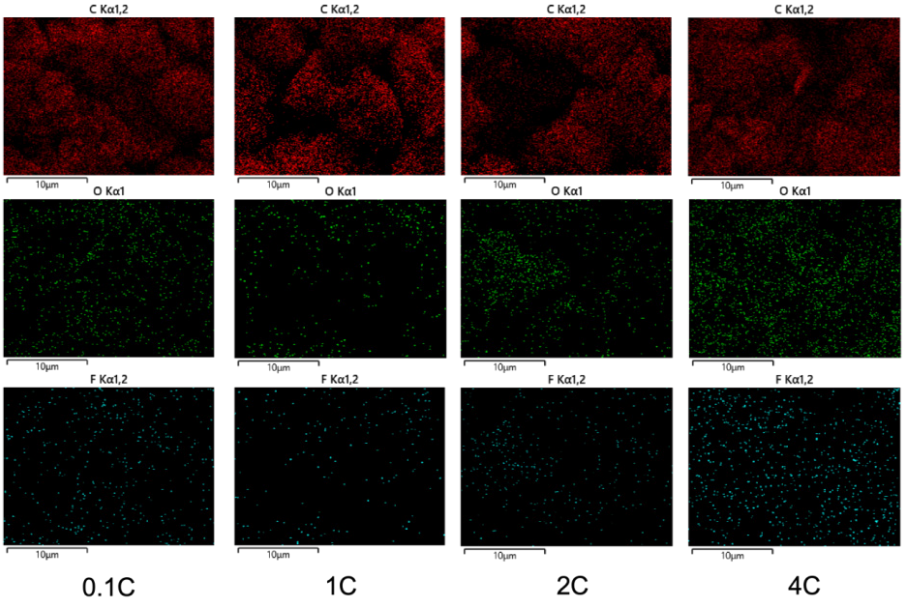

Figure 5. Representative EDS images of ex situ characterization of the structural evolution under varying degrees of lithium plating severity.

At Grade I, there is a slight reduction in the relative carbon contribution, whereas the presence of species containing oxygen and fluorine increases, which indicates the beginning of surface disturbance and electrolyte decomposition. This tendency is even more noticeable at Grade II, which means that the reaction products cover larger areas of the surface and that there is an increased strength of the interfacial reconstruction. At Grade III carbon is even more suppressed and oxygen and fluorine-containing species are much more enriched as expected with very serious surface chemical disturbance due to large-scale plating and parasitic reactions.

SEM and EDS confirm that the negative-electrode-potential-based framework is able to represent the real structural and chemical changes of the graphite anode at high rates of charge.

4. Conclusion

The severity-based lithium plating grading system was developed using the development of the negative-electrode potential in a three-electrode pouch cell. Operando monitoring indicated that higher charge rates cause the graphite anode to enter plating-susceptible low-potential areas at higher and increasingly lower potentials and thus indicate a higher risk of plating. Based on these criteria, lithium plating was divided into four categories: plating-free, mild, moderate, and severe. DEIS offered additional information about growing interfacial perturbation whereas SEM and EDS verified the same in terms of morphology and compositional changes of the graphite surface. The findings prove that the negative-electrode potential is a useful and mechanistically informative measure of severity-resolved lithium plating diagnosis and high-charging vulnerability evaluation.

Disclosure statement

The author declares no conflict of interest.

References

[1] Choi N, Yew K, Lee K, et al., 2006, Effect of Fluoroethylene Carbonate Additive on Interfacial Properties of Silicon Thin-Film Electrode. Journal of Power Sources, 161(2): 1254–9.

[2] Feng J, Zhang Z, Ci L, et al., 2015, Chemical Dealloying Synthesis of Porous Silicon Anchored by In Situ Generated Graphene Sheets as Anode Material for Lithium-Ion Batteries. Journal of Power Sources, 2015(287): 177–83.

[3] He X, Bresser D, Passerini S, et al., 2021, The Passivity of Lithium Electrodes in Liquid Electrolytes for Secondary Batteries. Nature Reviews Materials, 6(11): 1036–52.

[4] Liu X, Wang M, Cao R, et al., 2023, Review of Abnormality Detection and Fault Diagnosis Methods for Lithium-Ion Batteries. Automotive Innovation, 6(2): 256–67.

[5] Lu Y, Wang X, Mao S, et al., 2023, Smart Batteries Enabled by Implanted Flexible Sensors. Energy & Environmental Science, 16(6): 2448–63.

[6] Ma J, Yan H, Li B, et al., 2016, Tuning the Electronic Structure of the Metal-Oxygen Group by Silicon Substitution in Lithium-Rich Manganese-Based Oxides for Superior Performance. Journal of Physical Chemistry C, 120(25): 1342–6.

[7] Nie L, Chen S, Liu W, 2023, Challenges and Strategies of Lithium-Rich Layered Oxides for Li-Ion Batteries. Nano Research, 16(1): 391–402.

[8] Peled E, 1979, The Electrochemical Behavior of Alkali and Alkaline Earth Metals in Nonaqueous Battery Systems: The Solid Electrolyte Interphase Model. Journal of the Electrochemical Society, 126(12): 2047–51.

[9] Peng Y, Ding M, Zhang K, et al., 2024, Quantitative Analysis of the Coupled Mechanisms of Lithium Plating, SEI Growth, and Electrolyte Decomposition in Fast Charging Battery. Acs Energy Letters, 9(12): 6022–8.

[10] Rui X, Ren D, Liu X, et al., 2023, Distinct Thermal Runaway Mechanisms of Sulfide-based All-Solid-State Batteries. Energy & Environmental Science, 16(8): 3552–63.

[11] Tarascon J, Armand M, 2001, Issues and Challenges Facing Rechargeable Lithium Batteries. Nature, 414(6861): 359–67.

[12] Wan H, Xu J, Wang C, 2024, Designing Electrolytes and Interphases for High-Energy Lithium Batteries. Nature Reviews Chemistry, 8(1): 30–44.